Med

CellPress

Review

Tissue clearing and 3D reconstruction of digitized, serially sectioned slides provide novel insights into pancreatic cancer

Ashley L. Kiemen,[1,2,8] Alexander Ioannis Damanakis,[1,3,8] Alicia M. Braxton,[1,8] Jin He,[4] Daniel Laheru,[5] Elliot K. Fishman,[6] Patrick Chames,[7] Cristina Almagro Pérez,[2] Pei-Hsun Wu,[2] Denis Wirtz,[1,2] Laura D. Wood,[1,5,*] and Ralph H. Hruban[1,5,*]

SUMMARY

Pancreatic cancer is currently the third leading cause of cancer death in the United States. The clinical hallmarks of this disease include abdominal pain that radiates to the back, the presence of a hypoenhancing intrapancreatic lesion on imaging, and widespread liver metastases. Technologies such as tissue clearing and three-dimensional (3D) reconstruction of digitized serially sectioned hematoxylin and eosin-stained slides can be used to visualize large (up to 2- to 3-centimeter cube) tissues at cellular resolution. When applied to human pancreatic cancers, these 3D visualization techniques have provided novel insights into the basis of a number of the clinical characteristics of this disease. Here, we describe the clinical features of pancreatic cancer, review techniques for clearing and the 3D reconstruction of digitized microscope slides, and provide examples that illustrate how 3D visualization of human pancreatic cancer at the microscopic level has revealed features not apparent in 2D microscopy and, in so doing, has closed the gap between bench and bedside. Compared with animal models and 2D microscopy, studies of human tissues in 3D can reveal the difference between what can happen and what does happen in human cancers.

INTRODUCTION

Pancreatic cancer robs those diagnosed of hope.[1] It has been estimated that, globally, 495,773 people were diagnosed with pancreatic cancer in 2020 and that 466,003 died from the disease.[2] As bad as these statistics are, they appear to be getting worse. Rahib and colleagues have predicted that deaths from pancreatic cancer will become the second leading cause of cancer-related death in the United States by the year 2030.[3–5] New approaches to understanding, diagnosing, and treating this disease are needed.

Historically, pancreatic cancer has been diagnosed and studied using two-dimensional (2D) microscopy.[6,7] These studies in 2D significantly under sample the cancers. If the greatest dimension of the average surgically resected pancreatic cancer is 3 cm, and if the pathologist examines one 5-μm-thick hematoxylin and eosin (H&E)-stained slide section for every 1 cm of tumor, then pathologists examine less than 0.05% of the average surgically resected pancreatic cancer. This incomplete view has several implications. First, the connectivity of cancer cells is lost. Cancers that appear to be separate

[1]Department of Pathology, The Sol Goldman Pancreatic Cancer Research Center, The Johns Hopkins University School of Medicine, Baltimore, MD 21287, USA

[2]Department of Chemical & Biomolecular Engineering, The Johns Hopkins University, 3400 N Charles St, Baltimore, MD 21218, USA

[3]Department of General, Visceral, Cancer and Transplant Surgery, University Hospital of Cologne, Cologne, Germany

[4]Department of Surgery, The Sol Goldman Pancreatic Cancer Research Center, The Johns Hopkins University School of Medicine, Baltimore, MD 21287, USA

[5]Department of Oncology, The Sol Goldman Pancreatic Cancer Research Center, The Johns Hopkins University School of Medicine, Baltimore, MD 21287, USA

[6]Department of Radiology, The Sol Goldman Pancreatic Cancer Research Center, The Johns Hopkins University School of Medicine, Baltimore, MD 21287, USA

[7]Antibody Therapeutics and Immunotargeting Team, Aix Marseille University, CNRS, INSERM, Institut Paoli-Calmettes, CRCM, Marseille, France

[8]These authors contributed equally

*Correspondence: ldwood@jhmi.edu (L.D.W.), rhruban@jhmi.edu (R.H.H.)

https://doi.org/10.1016/j.medj.2022.11.009

Please cite this article in press as: Kiemen et al., Tissue clearing and 3D reconstruction of digitized, serially sectioned slides provide novel insights into pancreatic cancer, Med (2022), https://doi.org/10.1016/j.medj.2022.11.009

islands of neoplastic ducts embedded in stroma in 2D are, in fact, often contiguous branching 3D tubes of cancer cells.[8] Second, the prevalence of a feature such as vascular invasion will be underestimated as focal microscopic features are unlikely to be captured in the minuscule fraction of the cancer sampled. Third, relationships among cells are lost in thin sections unless the two cells coincidentally fall in the same 5-μm plane of section. For example, the relationship between an immune cell and a neoplastic cell cannot be appreciated unless the two cells are in the same plane of section.[9] Fourth, the exact point at which an event occurs is not identifiable in 2D slides. In 2D, we can observe cancer cells in a nerve, but we do not know at what point along the full length of that nerve the cells invaded the nerve. Recent technological advances in the microscopic visualization of human tissues in 3D make the visualization of even large volumes at the cellular level possible and, in so doing, overcome many of the limitations of 2D microscopy.

Here, we provide a brief clinical overview of pancreatic cancer, review two broad technologies for 3D visualization of cancers at the microscopic level, and then show how the 3D visualization of human pancreatic cancer has provided insight into clinically important issues. Looking forward, we envision that true 3D multiomic analyses of cancers on the subcellular level will soon revolutionize our understanding of cancer growth and metastasis.

CLINICAL

Signs and symptoms

Intractable abdominal pain, particularly severe pain that radiates to the back, is one of the most dominant symptoms experienced by patients with pancreatic cancer.[1,10,11] This pain has been linked to cancer cells invading nerves (perineural invasion), and, when carefully examined, perineural invasion can be found in virtually all pancreatic cancers.[10,12–15] Perineural invasion, in turn, has been associated with poor prognosis in patients with pancreatic cancer.[10,16] Many of the nerves in the pancreas arise in either the celiac plexus or the superior mesenteric plexus, and pancreatic cancers can grow along nerves into the connective tissues around the celiac and superior mesenteric arteries.[12,16,17] Local recurrence, often in the area of the celiac and superior mesenteric plexuses, occurs in 15%–25% of patients with pancreatic cancer who undergo surgical resection, and this local recurrence has been correlated with perineural invasion.[18–20] Local recurrence secondary to the involvement of nerves is such a significant problem that some have suggested that the standard surgery (pancreatoduodenectomy) should be extended to include the resection of these nerve plexuses.[21]

Signs and symptoms related to the obstruction of the pancreatic and bile ducts can also dominate the clinical picture for patients with pancreatic cancer. The main pancreatic duct and the distal common bile duct both pass through the head of the pancreas before they drain into the duodenum, and both ducts are often narrowed by cancers in the head of the gland.[22] Obstruction of the bile duct leads to jaundice, while obstruction of the pancreatic duct causes upstream chronic pancreatitis with loss of both exocrine and endocrine cells.[23,24]

Other signs and symptoms of pancreatic cancer include deep venous thromboses, pulmonary emboli, migratory venous thrombophlebitis, weight loss, and nausea.[25–27]

These signs and symptoms are non-specific, and most patients with pancreatic cancer are not diagnosed until after the disease has spread to other organs. The liver is

Please cite this article in press as: Kiemen et al., Tissue clearing and 3D reconstruction of digitized, serially sectioned slides provide novel insights into pancreatic cancer, Med (2022), https://doi.org/10.1016/j.medj.2022.11.009

the most common site of metastasis, and close to 80% of patients develop liver metastases.[28–30] The impact of this is devastating as the 5-year survival rate for patients with liver metastases is only 3%[31]

Diagnosis

Computed tomography (CT) can be performed to confirm the presence of a pancreatic lesion.[32] When intravenous contrast is given, the majority of pancreatic cancers are visualized as ill-defined hypoenhancing (relative to the adjacent normal pancreas) intrapancreatic masses.[32,33] Other imaging modalities include magnetic resonance imaging (MRI) and endoscopic ultrasound (EUS).[32] EUS has the advantages that a biliary stent can be placed in patients with obstructive jaundice and that biopsies for pathological examination and for molecular analyses can be obtained.[34,35] As a variety of neoplastic and non-neoplastic entities can form mass lesions in the pancreas, pathology is the "gold standard" in establishing the diagnosis.[6,7]

Pathology

Pancreatic cancers grossly form firm, white, ill-defined masses that replace pancreatic parenchyma.[6,7] At the microscopic level, when viewed in 2D, pancreatic cancers appear as individual glands haphazardly arranged in dense desmoplastic stroma.[6,7,36] One manifestation of this haphazard growth is the diagnostically helpful finding of a neoplastic gland immediately adjacent to a muscular vessel.[37] When examined with 2D microscopy, vascular invasion, including the invasion of lymphatic spaces as well as the invasion of veins, is identified in 65% of surgically resected pancreatic cancers.[6,7,38,39] As noted earlier, perineural invasion is seen microscopically in virtually all pancreatic cancers.[16]

Compared with other cancer types, the stroma is particularly dense in pancreatic cancers.[6,7,36] This stroma is rich with activated fibroblasts, dense collagen, and immune cells.[36,40]

Treatment

The optimal treatment for patients with pancreatic cancer depends on the stage of the disease. Surgery, the best hope for a cure, is indicated for patients with low-stage disease.[41] Close to 50% of surgically resected patients with stage T1 or T2 disease are alive 5 years after surgery.[42] Radiation therapy is often also given, particularly in the United States, to achieve better local control of the disease and for patients with locally advanced pancreatic cancer to shrink the cancer to the point where surgery is an option.[43]

Chemotherapy can be given before (neoadjuvant) and after (adjuvant) surgery or as a primary therapy in patients with advanced disease.[44] Chemotherapy is the mainstay of treatment for patients with advanced disease, and several drug combinations, including FOLFIRINOX (fluorouracil, irinotecan, leucovorin, oxaliplatin), gemcitabine/nab-paclitaxel, and nanoliposomal irinotecan/fluorouracil, have been shown to improve survival by 2 to 6 months in patients with metastatic pancreatic cancer compared with single-agent gemcitabine.[44] Several investigators have suggested that inadequate drug delivery to the cancers accounts for the poor response of pancreatic cancer to systemic chemotherapy.[36,45,46]

Despite improvements in survival for other cancer types over the past decade, the 5-year survival rate for patients diagnosed with pancreatic cancer in the United States is an abysmal 11%.[31,47]

Please cite this article in press as: Kiemen et al., Tissue clearing and 3D reconstruction of digitized, serially sectioned slides provide novel insights into pancreatic cancer, Med (2022), https://doi.org/10.1016/j.medj.2022.11.009

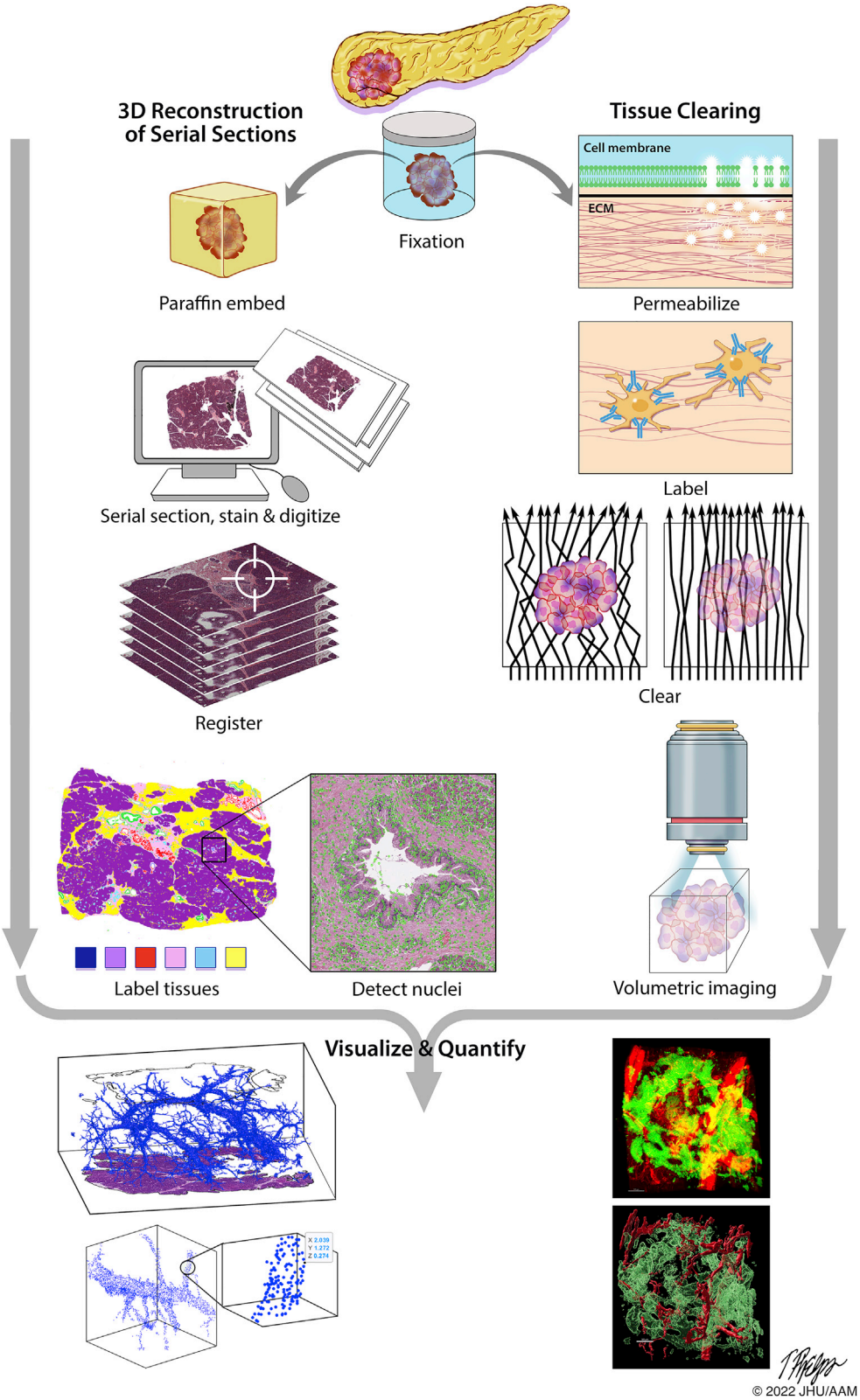

Figure 1. Two approaches to 3D histology include 3D reconstruction of serially sectioned slides (left side) and tissue clearing (right side)
3D reconstruction of serial sections includes fixing the tissue, embedding it (usually in paraffin), serially sectioning the block, and then digitizing the resultant slides. The digital images can then be registered and cell types identified using deep-learning techniques. Clearing includes fixation, permeabilizing the tissue to allow for the penetration of antibodies, labeling with antibodies, clearing, and then imaging using either light sheet or confocal microscopy. Both procedures can produce 3D datasets amendable to microscopic visualization and quantification of histology not apparent in 2D (bottom third).

Recent advances in 3D microscopy reveal features of pancreatic cancer that are not apparent in 2D microscopy.[48] These features provide clinically relevant insights into the dominant characteristics of pancreatic cancer, and it is hoped that these insights will translate to improved patient outcome.

TECHNIQUES FOR 3D MICROSCOPY

Improvements in tissue clearing, artificial intelligence (AI) and microscopy now make 3D visualization of large volumes of tissue at the cellular level possible.[49,50] Here, we present two techniques, clearing and the 3D reconstruction of serially sectioned and digitized microscope slides, each with strengths and weaknesses, that have been applied to the 3D visualization of human pancreatic cancer (Figure 1).[48,50–58]

Tissue clearing

The prerequisite to visualizing intact thick tissues is transparency, as light must be able to pass through the sample. While some specimens are nearly transparent and may be successfully imaged without clearing, many human and animal tissues, and especially dense, fibrous pancreatic cancers, need to be rendered transparent to enable optical sectioning using modern microscopy techniques. We therefore use the term "tissue clearing" when referring to 3D immunolabeling and optical visualization in this review.

Two distinct procedures are necessary for 3D microscopy using tissue clearing. First, cells and tissues of interest are labeled. The principles follow those of 2D immunofluorescence, with the additional complexity of needing to label antigens deeper in the tissues. To accomplish this deeper labeling, the extracellular matrix has to be permeabilized and cell membranes partially delipidated (Figure 1).[50,59] Human pancreatic cancer is especially challenging as it is densely fibrotic.[36,60] Permeabilization can be increased through a combination of detergents, collagenases, acids, denaturants, and temperature changes.[48,61–63] The cells are then labeled using long, up to weeks, antibody incubation times (Figure 1). As the size of antibodies determines their ability to penetrate tissues, nanobodies, which are small (~15 kDa versus monoclonal antibodies, which are ~150 kDa) single-domain antibodies found in Camelidae (alpaca, llama), are emerging as a versatile option.[64–67] In addition to immunolabeling, the autofluorescence properties of specific tissues and cells can be exploited to visualize structures without labeling.[48,68] Sources contributing to autofluorescence in the pancreas include nicotinamide adenine dinucleotide phosphate (NADPH), laminins, collagens, elastin, porphyrins, and lipofuscins.[68,69] Collagens and elastin account for the most intense autofluorescent signal in the pancreas, making autofluorescence a useful approach to visualizing vessels (as seen in Figure 2A and Videos S1 S2, S7). Furthermore, arteries can be distinguished from veins based on the characteristic intense autofluorescence of the elastic lamina in arteries (Videos S1 and S2). In the pancreas, excitation using a 488-nm light source can be used to highlight the autofluorescence, while autofluorescence is generally lower at higher excitation wave lengths (>640 nm).

Please cite this article in press as: Kiemen et al., Tissue clearing and 3D reconstruction of digitized, serially sectioned slides provide novel insights into pancreatic cancer, Med (2022), https://doi.org/10.1016/j.medj.2022.11.009

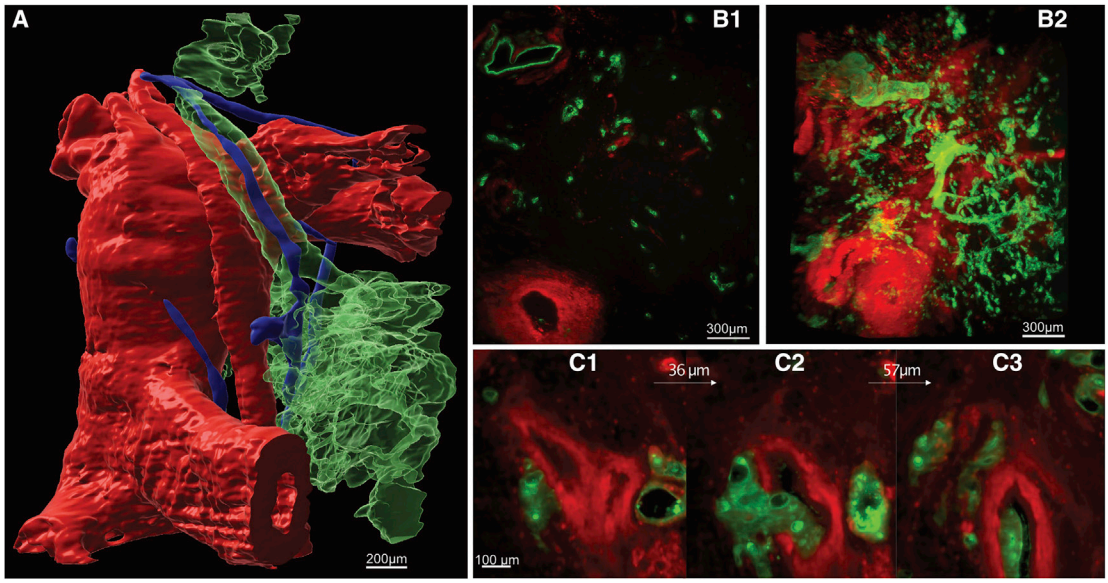

Figure 2. Tissue clearing of human pancreatic cancer revealing perineural invasion, 2D and 3D architecture of the invasive cancer, and vascular invasion

(A) Cleared human pancreatic cancer with surface rendering. Note the neoplastic cells (green) growing parallel to a vein (red, running down the center of the image from 12 o'clock to 6 o'clock) and its associated thicker artery (red, left side of the image). The neoplastic cells grow around a nerve (blue) and parallel to the vein. Videos S1 and S2 are paired videos.

(B) Cleared human pancreatic cancer reveals that isolated glands in 2D (B1) are actually often longer tubes of cancer cells in 3D (B2). Videos S3 and S4 are paired videos.

(C) Cleared human pancreatic cancer. Selected images at serial levels illustrate that vascular invasion (C2) can be missed (C1) in 2D. In C1, cancer cells (green) are seen growing next to, not in, the vessel (red). (C2) shows the point at which the cancer invades the vessel, and (C3) shows the same cancer growing inside the vessel. Video S7 is a paired video that highlights the focality of vascular invasion.

Light sheet microscopy, 3.2× (A), 6.4× (B), and 10× (C). Red is autofluorescence (A–C); green is labeling for carcinoembryonic antigen (A and C) or labeling for cytokeratin 19 (B); and blue is S-100 protein labeling (A). In (C), the z stack distance between the left and middle images is 36 μm, and the distance between the middle and right images is 57 μm.

The next step is to overcome the opaqueness of tissues so that the excitation and emission light can pass through the tissues.

Tissue clearing overcomes the opaqueness of tissues by creating tissues with a uniform refractive index (Figure 1).[49,50] Living organisms are composed of cells and tissues with varying refractive indexes. Water has a refractive index of 1.33, while the refractive index of lipids and proteins can range from 1.4 to 1.6.[49,70,71] Light bends as it passes from one medium into a medium with a different refractive index. As a result, complex heterogenous tissues become opaque. Tissue clearing overcomes this by reducing the heterogeneity of refractive indices in the tissues being studied.[49,70,71] This transparency can be achieved through aqueous- and solvent-based approaches.[62,72] For the human pancreas, the combination of dichloromethane and dibenzyl ether have proven to be highly effective.[48,59,62,73]

The final step is microscopy. The most commonly used techniques are light-sheet fluorescence microscopy (LSFM), optical projection tomography (OPT), and, for higher magnification, laser-scanning confocal microscopy or two-photon microscopy.[59,61–63,69,74] Each of these techniques has strengths and weaknesses.

LSFM (Figure 2; Videos S1–S4 and S7) uses laser beams to illuminate a plane of adjustable thickness within the tissue.[75] A synonym for light-sheet miroscopy is, therefore, selective-plane illumination microscopy (SPIM). The objective capturing

light emitted from excited fluorophores within the tissue is placed orthogonal to the laser beams and has a high numerical aperture.[75] Filters are selected to match the emission spectrum of the fluorophores, and each excitation channel (wavelength of the laser) is recorded separately. Exposure times will vary depending on the thickness of the tissue, fluorophore signal intensity, and laser intensity, but it generally takes between 50 and 220 ms to record a single image (times are doubled when using a two-sided laser, which results in better light penetration in larger tissues). The sample can then be optically sectioned by moving the tissue through the plane of light. Depending on the size of the sample and the number of channels recorded, the acquisition time for an entire specimen can easily reach 2 to 5 h. Long imaging times are possible as the low laser intensities used with LSFM typically do not produce significant photobleaching (the permanent alteration of a fluorophore, leading to loss of fluorescence signal). A downside of LSFM is that the axial resolution is limited to ~1 μm, which is worse than the lateral resolution.[75]

OPT has also been widely used to visualize labeled and cleared samples. Technically, OPT is comparable to medical CT, only OPT uses ultraviolet, visible, and near-infrared photons instead of X-ray photons.[76] Image contrast is achieved through absorption/scattering in transmission OPT, while it is achieved through fluorescence in emission OPT. The sample is usually rotated, allowing for the acquisition of multiple 2D images from different angles (2D projections). These 2D images are then used to reconstruct 3D volumes; however, the reconstruction algorithms add complexity to OPT 3D microscopy.[77] OPT and LSFM can often complement each other. In general, OPT is more suitable for larger samples recorded at lower magnification, while LSFM, although limited in axial resolution, can achieve higher-resolution images of smaller samples.

Laser scanning confocal microscopy employs an array of pinholes to focus both the excitation (point illumination) light and the emission light.[78] The field of view is then scanned point by point.[78] Adaptation of the point of focus allows for optical sectioning and the subsequent creation of 3D volumes at extremely high (150×) magnifications. The penetration of excitation light and the detection of emitted light are, however, limited, making laser scanning confocal microscopy not suitable for thicker tissues.[78] Two-photon microscopy is another point-scanning fluorescent microscopy technique that reduces photobleaching by using two photons of higher wavelength instead of a single photon of lower wavelength.[79] Photons are emitted almost synchronously, only around 50 femtoseconds apart, which results in the same excitation signal but with significantly less photobleaching and reduced scattering in deeper tissue sections. These scanning fluorescent microscopy techniques come with a trade-off, as although they can generate extremely high-resolution images, the field of view is generally limited compared with LSFM.

The datasets produced by these various microscopy techniques can be further processed using surface or spot rendering, enabling shape and co-localization analyses. Pattern recognition algorithms can also be applied to trace complex neuronal or vascular networks and to identify connections that may not be apparent to the human eye.[80]

3D reconstruction of digitized serial microscope slides

Several methods have been developed to create 3D reconstructions of microscopic slides from serially sectioned samples.[52–57] Tissues are typically serially sectioned, the slides digitized, and then the digital images are registered to create digital tissue volumes (Figure 1).[52–57] Manual segmentation or deep learning can then be used to label components in the digitized images (Figure 1).[52,81] In the pancreas, as many as ten

Please cite this article in press as: Kiemen et al., Tissue clearing and 3D reconstruction of digitized, serially sectioned slides provide novel insights into pancreatic cancer, Med (2022), https://doi.org/10.1016/j.medj.2022.11.009

Table 1. A comparison of two methods for visualizing human pancreatic cancer in 3D at the microscopic level

Feature	Clearing	3D reconstruction of serial microscope slides
Size of sample that can be studied	entire human brains have been studied	determined by the size of the microscope slides (x,y plane) and by number of sections cut (z plane).
Application to densely fibrotic pancreatic cancer	limited by poor antibody penetration	not limited by antibody penetration; uniform resolution even deep in tissues
Number of tissue types that can be studied in human pancreatic cancer	usually three or four fluorophores (antibodies) plus autofluorescence of vessels	10+ distinct tissues labeled with CODA
Application of other technologies such as sequencing	limited by the harsh chemicals used	limited only to technologies applicable to formalin-fixed, paraffin-embedded tissues
Cost	$	$$$ (proportionate to number of slides sectioned)
Time to process one sample	4–50 days (depending on protocol used, use of unconjugated or conjugated antibodies/ nanobodies); upscaling is easily possible as samples can be run in parallel	sectioning/scanning: 1 week; computer processing: 1 week
Quality of images	visually stunning	more easily related to standard H&E-stained sections
Nuclear detail	often lost; propidium iodide can be used to detect nuclei in labelled cells, but details are often lost	retained

structures (normal ductal epithelium, pancreatic precancers, pancreatic cancer, islets of Langerhans, vessels, nerves, acini, stroma, lymph nodes, and fat) have been labeled at a resolution of 1–2 μm.[52] Unused intervening sections can be used for immunohistochemistry, imaging mass cytometry, somatic sequencing, and spatial transcriptomics, creating 3D integrations of histologic, gene, protein, and immune features.[52,82–88]

In this review, when describing the 3D reconstructions of microscopic slides, we will focus on the approach called CODA, as CODA has been applied extensively to human pancreatic tissues.[52] CODA relies on four major steps: image registration, cell detection, tissue segmentation, and data visualization (Figure 1). The registration step maximizes the 2D cross correlation of pixel intensity between pairs of images to correct for the rotation, translation, folding, splitting, and stretching of tissues that occur during microtomy. The cell detection step uses color deconvolution to isolate the hematoxylin channel, and 2D peaks in this channel are then used to define nuclear coordinates. The tissue identification step then uses a small dataset of manual annotations to train a deep-learning semantic segmentation algorithm. Once trained, the algorithm can efficiently label, to a resolution of 1 μm, microanatomical structures in the pancreas such as ductal epithelium, acinar tissue, cancer, and vessels. Finally, the image registration, cell detection, and tissue segmentation are integrated to create 3D renderings of pancreas microanatomy at large scale (up to cm^3) while maintaining single-cell resolution.

Clearing and 3D reconstruction of digitized serial microscope slides are not mutually exclusive as, after imaging, cleared tissues can be washed, formalin fixed and paraffin embedded, and then serially sectioned for 3D reconstruction.[48,69,89] Although the resultant images may have retraction artifacts, they can, nonetheless, be useful in validating observations made in cleared tissues.[48]

Strengths and weaknesses

The primary differences between clearing and 3D reconstruction of serial microscope slides relate to the size of tissues, and the number of markers, that can be examined (Table 1).

Clearing can be used to visualize whole organs, including entire human brains.[59,90] However, clearing relies on antibody penetration, and antibodies do not penetrate deeply into densely fibrotic tissues such as human pancreatic cancer.[48,62] By

Table 2. Comparison of resolutions and sample sizes for human pancreatic cancer

	Light sheet fluorescence microscopy	3D reconstruction of serial microscope slides
Lateral resolution	>0.3 mm	~0.25 (40×) or ~0.5 mm (20×)
Axial resolution	>1 mm	>4 mm (tissue section thickness)
Sample size size limit in x, y direction	~15 × 15 mm^2 (LSFM)	~20 × 50 mm^2
Sample size size limit in x, y direction	<10 mm	unlimited
Z continuity	good	moderate

contrast, the potential size of the tissue that can be reconstructed using 3D reconstruction of microscope slides is limited only by the size of the slides (x,y direction) and by the number of sections cut (axial, or z direction).[52] Additionally, since the tissue is sectioned in the generation of serial microscope slides, all tissue is visualized homogeneously; there are no "dark" regions as happens when there is poor antibody penetration using clearing. Several approaches have been developed to overcome the limitations of antibody penetration, including first sectioning larger samples into smaller slabs, clearing and labeling the smaller slabs individually, and then stitching the visualized slabs together using imaging software.[63] At the other end of the scale, tissue clearing can also be applied to organoids alone or be combined with other tissue engineering approaches, including tissue-engineered microvessels.[74,91] The sizes of tissue that can be examined and resolutions that can be achieved by the two approaches are summarized in Table 2.

In 3D reconstruction of serial microscope slides, AI-based segmentation allows rapid identification of multiple tissue components that are distinguishable in H&E-stained sections (in the human pancreas, this includes 10 labels with CODA).[52,81] By contrast, only four or five components are typically identified with clearing: three or four using antibodies with different fluorophores, and one taking advantage of distinct patterns of autofluorescence.[48,52,69]

The main advantage of 3D reconstruction of serial microscope slides is that because unstained intervening slides are available, this approach is readily integrable with any technique that can be applied to formalin-fixed, paraffin-embedded tissues, such as immunohistochemistry, image mass cytometry, somatic sequencing, and spatial transcriptomics.[52,86,87] This level of integration is generally not possible with clearing because of the harsh chemicals employed.

INSIGHTS FROM 3D

The 3D visualization of human pancreatic tissues has provided clinically important insights into pancreas pathology that are not apparent in 2D (Figure 3; Table 3). In standard 2D H&E-stained microscope slides, pancreatic cancer appears as isolated glands haphazardly scattered in desmoplastic stroma (Figures 2B1 and 3E; Video S3). When visualized in 3D, it is clear that invasive pancreatic cancer cells, in fact, can grow as continuous branching tubes (Figures 2B2 and 3E; Video S4).[8] These tubes do not grow randomly but sometimes grow along tissue planes that are not appreciated in 2D sections. While the collagen fibers in the stroma of the pancreas appear disorganized when viewed in 2D, in the plethora of planes visualizable in 3D, these fibers can be shown to be well oriented, particularly around pancreatic ducts and vessels (Figures 3A and 4A; Video S5).[48,52,92–96] Benias and colleagues recently described previously unrecognized interstitial spaces lined by cells expressing endothelial markers between well-oriented collagen fibers around vessels and ducts

Please cite this article in press as: Kiemen et al., Tissue clearing and 3D reconstruction of digitized, serially sectioned slides provide novel insights into pancreatic cancer, Med (2022), https://doi.org/10.1016/j.medj.2022.11.009

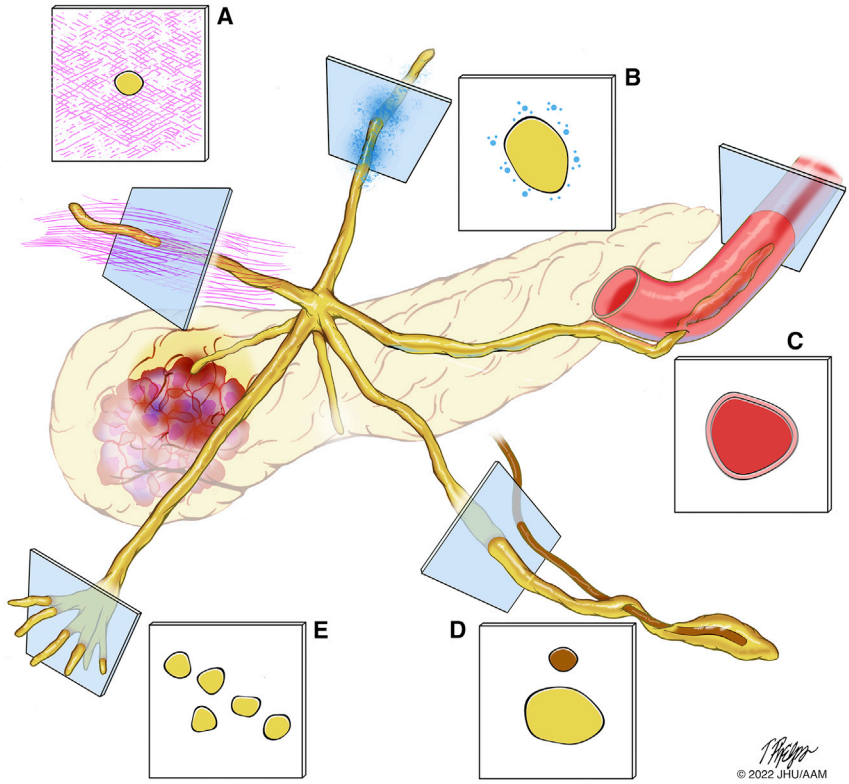

Figure 3. Illustration highlighting some features identifiable in 3D microscopy that would be missed/incorrectly interpreted in 2D histology (blue and clear slices)

(A) Collagen fibers that appear haphazardly aligned in 2D can be seen to have an organization in 3D.

(B) Counts of immune cells in in 2D only sample a small portion of what is shown to be a heterogenous immune infiltrate in 3D.

(C) Venous invasion is almost ubiquitous in 3D; however, it can easily be missed in 2D sections.

(D) The extent of perineural invasion visualized in 3D can be underestimated in 2D microscopy.

(E) Invasive carcinoma appears as isolated glands in 2D is often shown, in fact, to be contiguous branching tubules when viewed in 3D.

in the biliary tree, and they hypothesized that these spaces are present widely in the body and that these spaces are a pathway for cancer spread.[97] The patterns of growth observed in 3D suggest that pancreatic cancer may invade using the microchannels identified by Benias. Indeed, well-oriented collagen fibers and interstitial spaces in the connective tissue surrounding veins in the pancreas may explain the propensity of pancreatic cancer to grow parallel to veins (Figures 2A and 3C; Videos S1 and S2).[48] What appears as random in 2D, when studied in 3D, is found to be a propensity for growth parallel to vessels.[48]

The growth of pancreatic cancer parallel to vessels may, in turn, explain the high prevalence of venous invasion in pancreatic cancer. Venous invasion is observed in 60%–65% of surgically resected pancreatic cancers studied in 2D, but when studied in 3D, venous invasion can be identified in nearly 100% of the cancers (Figures 2C and 3C; Video S7).[38,39,51] The ubiquitous presence of venous invasion in even low-stage pancreatic cancers has important clinical implications. First, since the veins of the pancreas drain into the liver, venous invasion may explain the high prevalence of liver metastases and, ultimately, why pancreatic cancer is so deadly.[98] Second,

Please cite this article in press as: Kiemen et al., Tissue clearing and 3D reconstruction of digitized, serially sectioned slides provide novel insights into pancreatic cancer, Med (2022), https://doi.org/10.1016/j.medj.2022.11.009

Table 3. Comparison of clinical correlates of 2D and 3D microscopy

Clinical feature	2D microscopy	3D microscopy
Pain	perineural invasion, visualized for a short distance	perineural invasion, visualized for a longer distances (>4 mm)
Hypoenhacement on imaging	desmoplastic stroma	venous invasion resulting in reduced outflow, which, in turn, diminishes inflow
Local dissemination of disease	perineural invasion	perineural invasion and continuous and discontinuous intravenous spread
Propensity for metastases to the liver	unclear	venous invasion is ubiquitous
Pathology diagnosis	gland next to vessel is a diagnostic feature, likely secondary to haphazard growth of the cancer cells	carcinoma specifically grows in well-oriented collagen planes and parallel to veins
Screening/early detection	single cross section of pancreatic intraepithelial neoplasia lesions	size of precursor lesions can be determined when contained in a tissue block, and they can be studied using a variety of ancillary technologies

because veins thrombose in areas of venous invasion, venous outflow from pancreatic cancers will be reduced.[38] With diminished outflow, the inflow of blood into the tumor will also be reduced. Venous invasion may therefore also contribute to the hypoenhancement on imaging and the poor delivery of systemic chemotherapies to pancreatic cancers.[38,98]

The high prevalence of perineural invasion, noted in 2D studies, has also been observed in 3D studies. In 3D, one can appreciate better the length of growth of the cancer along nerves.[10,52] Perineural invasion of 2,500 μm has been reported in 2D histologic slides, while in 3D, distances as great as 4 mm are readily visualizable (Figures 3D and 5A; Video S8).[10,99] These distances highlight the role of perineural invasion in local spread of disease and therefore in local recurrence.[18,19,99] Similarly, 3D examination of foci of venous invasion have identified foci in which cancer cells grow in continuity inside the vein for 2 mm before growing out into the stroma (Figure 5B).[52] These findings highlight venous invasion as a mechanism of intraparenchymal spread of pancreatic cancer.

Studies using 3D microscopy, because they can be used to identify the exact point at which a process occurs, can also help advance our understanding of disease mechanisms (Figure 5; Video S8).[52] For example, studies of the "moment of venous invasion" using tissue clearing have shown that epithelial-to-mesenchymal transition is only transient during vascular invasion.[51]

3D analyses have also uncovered flaws in the histologic classification of precursor lesions. In the current classification system, based on 2D microscopy, pancreatic intraepithelial neoplasia (PanIN) lesions are distinguished from intraductal papillary mucinous neoplasms (IPMNs) based on the size of the lesion.[100,101] PanINs are, by definition, <0.5 cm, while IPMNs are, by definition, ≥1 cm.[100,101] However, some lesions that meet diagnostic criteria for a PanIN in 2D (they are <0.5 cm in greatest dimension in the plane that they happened to be sectioned), when visualized in 3D, are found to involve >1 cm of duct and thus meet the size threshold for an IPMN (Figure 4B).[52] A classification system based on volumes, as is done with CT, would allow for lesion classification independent of the plane of section.

When lesions are entirely confined to a block of tissue, 3D analyses can also be to quantify the number of cells in that lesion.[52] Since PanINs and other precursors are a target for early detection efforts, understanding the exact size of PanINs and the number of cells in each PanIN will inform efforts to develop early detection tests.

Please cite this article in press as: Kiemen et al., Tissue clearing and 3D reconstruction of digitized, serially sectioned slides provide novel insights into pancreatic cancer, Med (2022), https://doi.org/10.1016/j.medj.2022.11.009

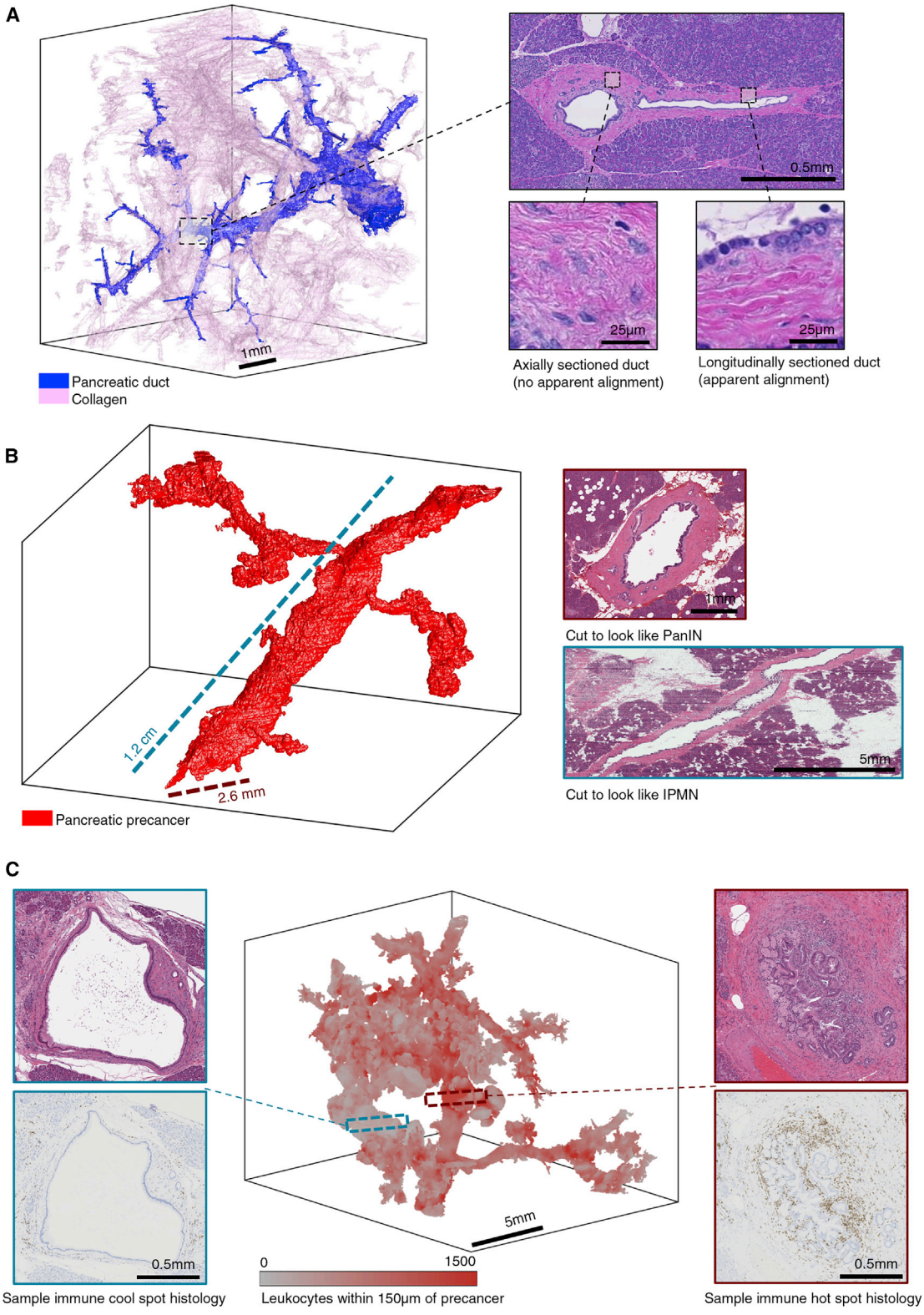

Please cite this article in press as: Kiemen et al., Tissue clearing and 3D reconstruction of digitized, serially sectioned slides provide novel insights into pancreatic cancer, Med (2022), https://doi.org/10.1016/j.medj.2022.11.009

Figure 4. 3D reconstructions of serially sectioned human pancreas using CODA

(A) Note how the collagen fibers in one plane appear poorly aligned and in another appear well aligned.

(B) The intraductal precursor lesion (red) measures 1.2 cm in one plane and 2.6 mm in another. If measured as 2.6 mm, the lesion would be classified as pancreatic intraepithelial neoplasia (PanIN), but if measured as 1.2 cm, it would be classified as an intraductal papillary mucinous neoplasm.

(C) The intervening unstained sections of a human pancreatic intraepithelial lesion were immunolabeled for CD45. In 3D, the intensity of the inflammatory infiltrate can be seen to range from minimal (left, blue box) to intense (right, red box).

(A and B) H&E. (C) Immunolabeling for CD45. Videos S5 and S6 are paired videos.

The most significant advantage of CODA is that only every third slide has to be used to generate the 3D images.[52] The two intervening slides can be used for molecular or immunolabeling studies.[86] A lesion can be identified in 3D, and then the intervening unstained slides of that lesion can be laser-capture microdissected and genetically sequenced, providing a 3D map of somatic mutations in the lesion. An understanding of the 3D architecture of somatic genetic alterations in complex branching and bending structures is needed to define molecular heterogeneity.

Similarly, intervening unstained sections can be used for immunolabeling, providing a 3D architecture of the immune reaction associated with a specific lesion (Figures 3B and 4C; Video S6).[9,86]

SUMMARY AND CONCLUSIONS

Visualizing human pancreatic cancers in three dimensions at the microscopic level has provided insights into the biology and clinical behavior human pancreatic cancer.[48,51,52] We envision two advances that will transform this field even further. First, as spatial transcriptomics technologies are optimized for formalin-fixed, paraffin-embedded tissues, detailed 3D spatial transcriptomics will soon be possible.[102,103] Second, as the resolution of clinical imaging techniques such as CT and MRI, improve, we foresee the direct, one-to-one correlation of 3D clinical

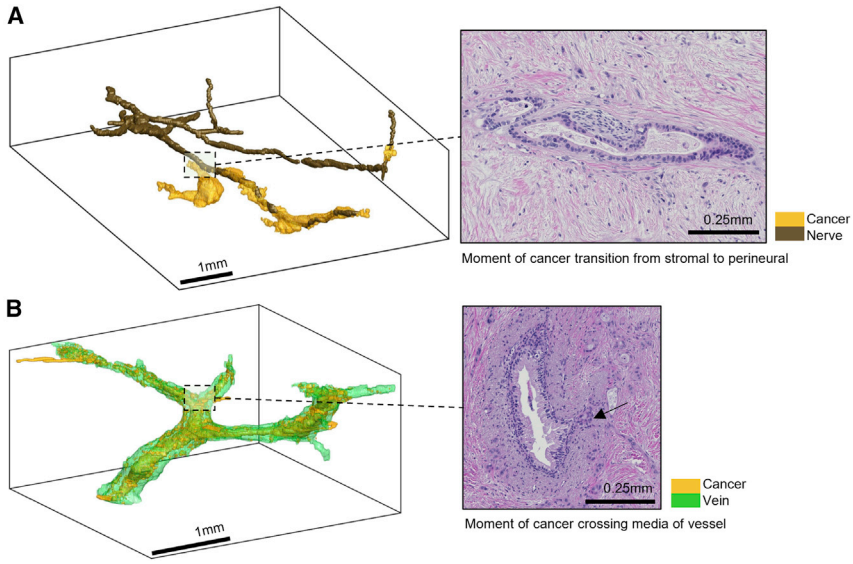

Figure 5. 3D reconstructions of serially sectioned human pancreas using CODA

(A) Highlighted invasive carcinoma (yellow) invading a nerve (brown) and then extending for a distance of 4 mm along the nerve. Note that the "moment" the cancer invades the nerve can be identified in this 3D visualization (right). Video S8 is a paired video.

(B) The invasive carcinoma (yellow) extensively grows within a vein (green) for a distance of at least 2 mm. Seven points can be identified where neoplastic cells cross the media of the vessel.

imaging with 3D microscopy.[104,105] AI will only increase the impact and speed the rate of advance of these analyses.[106]

The earth is not flat. Neither are human tissues.

SUPPLEMENTAL INFORMATION

Supplemental information can be found online at https://doi.org/10.1016/j.medj.2022.11.009.

ACKNOWLEDGMENTS

The authors thank the Michael Rolfe Foundation; the Sol Goldman Pancreatic Cancer Research Center; the Troper-Wojcicki Foundation; the Joseph C. Monastra Foundation; and the Gerald O Mann Charitable Foundation (Harriet and Allan Wulfstat, trustees). Support was provided from the National Cancer Institute (U54CA143868 to D.W. and P.-H.W. and U54CA268083 to D.W., P.-H.W., A.K., and L.D.W.) and the National Institute on Aging (U01AG060903 to D.W. and P.-H.W.).

AUTHOR CONTRIBUTIONS

A.K., A.I.D., L.D.W, and R.H.H. prepared the first draft of the manuscript. All authors reviewed, edited, and agreed to submit the manuscript, read and approved the final draft, and take full responsibility of its content.

DECLARATION OF INTERESTS

The authors declare no competing interests.

REFERENCES

1. Wolfgang, C.L., Herman, J.M., Laheru, D.A., Klein, A.P., Erdek, M.A., Fishman, E.K., and Hruban, R.H. (2013). Recent progress in pancreatic cancer. CA. Cancer J. Clin. *63*, 318–348.

2. Sung, H., Ferlay, J., Siegel, R.L., Laversanne, M., Soerjomataram, I., Jemal, A., and Bray, F. (2021). Global cancer statistics 2020: GLOBOCAN estimates of incidence and mortality worldwide for 36 cancers in 185 countries. CA. Cancer J. Clin. *71*, 209–249.

3. Rahib, L., Smith, B.D., Aizenberg, R., Rosenzweig, A.B., Fleshman, J.M., and Matrisian, L.M. (2014). Projecting cancer incidence and deaths to 2030: the unexpected burden of thyroid, liver, and pancreas cancers in the United States. Cancer Res. *74*, 2913–2921.

4. Carioli, G., Malvezzi, M., Bertuccio, P., Boffetta, P., Levi, F., La Vecchia, C., and Negri, E. (2021). European cancer mortality predictions for the year 2021 with focus on pancreatic and female lung cancer. Ann. Oncol. *32*, 478–487.

5. Rahib, L., Wehner, M.R., Matrisian, L.M., and Nead, K.T. (2021). Estimated projection of US cancer incidence and death to 2040. JAMA Netw. Open *4*, e214708.

6. Bosman, F.T., Carneiro, F., Hruban, R.H., and Theise, N.D. (2010). WHO Classification of Tumours of the Digestive System, 4th Edition (International Agency for Research on Cancer).

7. Hruban, R.H., Pitman, M.B., and Klimstra, D.S. (2007). Tumors of the Pancreas (American Registry of Pathology).

8. Yoshizawa, T., Hong, S.M., Jung, D., Noë, M., Kiemen, A., Wu, P.H., Wirtz, D., Hruban, R.H., Wood, L.D., and Oshima, K. (2020). Three-dimensional analysis of extrahepatic cholangiocarcinoma and tumor budding. J. Pathol. *251*, 400–410.

9. Lin, Y.Y., Wang, L.C., Hsieh, Y.H., Hung, Y.L., Chen, Y.A., Lin, Y.C., Lin, Y.Y., and Chou, T.Y. (2022). Computer-assisted three-dimensional quantitation of programmed death-ligand 1 in non-small cell lung cancer using tissue clearing technology. J. Transl. Med. *20*, 131.

10. Schorn, S., Demir, I.E., Haller, B., Scheufele, F., Reyes, C.M., Tieftrunk, E., Sargut, M., Goess, R., Friess, H., and Ceyhan, G.O. (2017). The influence of neural invasion on survival and tumor recurrence in pancreatic ductal adenocarcinoma - a systematic review and meta-analysis. Surg. Oncol. *26*, 105–115.

11. Lohse, I., and Brothers, S.P. (2020). Pathogenesis and treatment of pancreatic cancer related pain. Anticancer Res. *40*, 1789–1796.

12. Bapat, A.A., Hostetter, G., Von Hoff, D.D., and Han, H. (2011). Perineural invasion and associated pain in pancreatic cancer. Nat. Rev. Cancer *11*, 695–707.

13. Ceyhan, G.O., Demir, I.E., Altintas, B., Rauch, U., Thiel, G., Müller, M.W., Giese, N.A., Friess, H., and Schäfer, K.H. (2008). Neural invasion in pancreatic cancer: a mutual tropism between neurons and cancer cells. Biochem. Biophys. Res. Commun. *374*, 442–447.

14. Chatterjee, D., Katz, M.H., Rashid, A., Wang, H., Iuga, A.C., Varadhachary, G.R., Wolff, R.A., Lee, J.E., Pisters, P.W., Crane, C.H., et al. (2012). Perineural and intraneural invasion in posttherapy pancreaticoduodenectomy specimens predicts poor prognosis in patients with pancreatic ductal adenocarcinoma. Am. J. Surg. Pathol. *36*, 409–417.

15. Liang, D., Shi, S., Xu, J., Zhang, B., Qin, Y., Ji, S., Xu, W., Liu, J., Liu, L., Liu, C., et al. (2016). New insights into perineural invasion of pancreatic cancer: more than pain. Biochim. Biophys. Acta *1865*, 111–122.

16. Mitsunaga, S., Hasebe, T., Kinoshita, T., Konishi, M., Takahashi, S., Gotohda, N., Nakagohri, T., and Ochiai, A. (2007). Detail histologic analysis of nerve plexus invasion in invasive ductal carcinoma of the pancreas and its prognostic impact. Am. J. Surg. Pathol. *31*, 1636–1644.

17. Hameed, M., Hameed, H., and Erdek, M. (2010). Pain management in pancreatic cancer. Cancers *3*, 43–60.

18. Groot, V.P., Rezaee, N., Wu, W., Cameron, J.L., Fishman, E.K., Hruban, R.H., Weiss, M.J., Zheng, L., Wolfgang, C.L., and He, J. (2018). Patterns, timing, and predictors of recurrence following pancreatectomy for pancreatic ductal adenocarcinoma. Ann. Surg. *267*, 936–945.

19. Furuhashi, S., Sakaguchi, T., Murakami, T., Fukushima, M., Morita, Y., Ikegami, K., Kikuchi, H., Setou, M., and Takeuchi, H. (2020). Tenascin C in the tumor-nerve microenvironment enhances perineural invasion and Correlates with locoregional recurrence in pancreatic ductal adenocarcinoma. Pancreas *49*, 442–454.

20. Conroy, T., Hammel, P., Hebbar, M., Ben Abdelghani, M., Wei, A.C., Raoul, J.L., Choné, L., Francois, E., Artru, P., Biagi, J.J., et al. (2018). FOLFIRINOX or gemcitabine as adjuvant therapy for pancreatic cancer. N. Engl. J. Med. *379*, 2395–2406.

21. Klotz, R., Hackert, T., Heger, P., Probst, P., Hinz, U., Loos, M., Berchtold, C., Mehrabi, A., Schneider, M., Müller-Stich, B.P., et al. (2022). The TRIANGLE operation for pancreatic head and body cancers: early postoperative outcomes. HPB *24*, 332–341.

22. Cohen, J., Sawhney, M.S., Pleskow, D.K., Chuttani, R., Patel, N.J., Sheridan, J., and Berzin, T.M. (2014). Double-duct sign in the era of endoscopic ultrasound: the prevalence of occult pancreaticobiliary malignancy. Dig. Dis. Sci. *59*, 2280–2285.

23. Chari, S.T., Leibson, C.L., Rabe, K.G., Timmons, L.J., Ransom, J., de Andrade, M., and Petersen, G.M. (2008). Pancreatic cancer-associated diabetes mellitus: prevalence and temporal association with diagnosis of cancer. Gastroenterology *134*, 95–101.

24. Pannala, R., Basu, A., Petersen, G.M., and Chari, S.T. (2009). New-onset diabetes: a potential clue to the early diagnosis of pancreatic cancer. Lancet Oncol. *10*, 88–95.

25. Epstein, A.S., Soff, G.A., Capanu, M., Crosbie, C., Shah, M.A., Kelsen, D.P., Denton, B., Gardos, S., and O'Reilly, E.M. (2012). Analysis of incidence and clinical outcomes in patients with thromboembolic events and invasive exocrine pancreatic cancer. Cancer *118*, 3053–3061.

26. Khorana, A.A., Mackman, N., Falanga, A., Pabinger, I., Noble, S., Ageno, W., Moik, F., and Lee, A.Y.Y. (2022). Cancer-associated venous thromboembolism. Nat. Rev. Dis. Primers *8*, 11.

27. Seoud, T., Syed, A., Carleton, N., Rossi, C., Kenner, B., Quershi, H., Anand, M., Thakkar, P., and Thakkar, S. (2020). Depression before and after a diagnosis of pancreatic cancer: results from a national, population-based study. Pancreas *49*, 1117–1122.

28. Yachida, S., and Iacobuzio-Donahue, C.A. (2009). The pathology and genetics of metastatic pancreatic cancer. Arch. Pathol. Lab Med. *133*, 413–422.

29. Tanaka, M., Mihaljevic, A.L., Probst, P., Heckler, M., Klaiber, U., Heger, U., Büchler, M.W., and Hackert, T. (2019). Meta-analysis of recurrence pattern after resection for pancreatic cancer. Br. J. Surg. *106*, 1590–1601.

30. Zambirinis, C.P., Midya, A., Chakraborty, J., Chou, J.F., Zheng, J., McIntyre, C.A., Koszalka, M.A., Wang, T., Do, R.K., Balachandran, V.P., et al. (2022). Recurrence after resection of pancreatic cancer: can radiomics predict patients at greatest risk of liver metastasis? Ann. Surg Oncol. *29*, 4962–4974.

31. Siegel, R.L., Miller, K.D., Fuchs, H.E., and Jemal, A. (2022). Cancer statistics, 2022. CA A Cancer J. Clin. *72*, 7–33.

32. Chu, L.C., Goggins, M.G., and Fishman, E.K. (2017). Diagnosis and detection of pancreatic cancer. Cancer J. *23*, 333–342.

33. Chu, L.C., Park, S., Kawamoto, S., Yuille, A.L., Hruban, R.H., and Fishman, E.K. (2021). Pancreatic cancer imaging: a new look at an old problem. Curr. Probl. Diagn. Radiol. *50*, 540–550.

34. Habib, J.R., Zhu, Y., Yin, L., Javed, A.A., Ding, D., Tenior, J., Wright, M., Ali, S.Z., Burkhart, R.A., Burns, W., et al. (2021). Reliable detection of somatic mutations for pancreatic cancer in endoscopic ultrasonography-guided fine needle aspirates with next-generation sequencing: implications from a prospective cohort study. J. Gastrointest. Surg. *25*, 3149–3159.

35. Kitano, M., Yoshida, T., Itonaga, M., Tamura, T., Hatamaru, K., and Yamashita, Y. (2019). Impact of endoscopic ultrasonography on diagnosis of pancreatic cancer. J. Gastroenterol. *54*, 19–32.

36. Whittle, M.C., and Hingorani, S.R. (2019). Fibroblasts in pancreatic ductal adenocarcinoma: biological mechanisms and therapeutic targets. Gastroenterology *156*, 2085–2096.

37. Sharma, S., and Green, K.B. (2004). The pancreatic duct and its arteriovenous relationship: an underutilized aid in the diagnosis and distinction of pancreatic adenocarcinoma from pancreatic intraepithelial neoplasia. A study of 126 pancreatectomy specimens. Am. J. Surg. Pathol. *28*, 613–620.

38. Hong, S.M., Goggins, M., Wolfgang, C.L., Schulick, R.D., Edil, B.H., Cameron, J.L., Handra-Luca, A., Herman, J.M., and Hruban, R.H. (2012). Vascular invasion in infiltrating ductal adenocarcinoma of the pancreas can mimic pancreatic intraepithelial neoplasia: a histopathologic study of 209 cases. Am. J. Surg. Pathol. *36*, 235–241.

39. Yamada, M., Sugiura, T., Okamura, Y., Ito, T., Yamamoto, Y., Ashida, R., Sasaki, K., Nagino, M., and Uesaka, K. (2018). Microscopic venous invasion in pancreatic cancer. Ann. Surg Oncol. *25*, 1043–1051.

40. Grünwald, B.T., Devisme, A., Andrieux, G., Vyas, F., Aliar, K., McCloskey, C.W., Macklin, A., Jang, G.H., Denroche, R., Romero, J.M., et al. (2021). Spatially confined sub-tumor microenvironments in pancreatic cancer. Cell *184*, 5577–5592.e18.

41. He, J., Ahuja, N., Makary, M.A., Cameron, J.L., Eckhauser, F.E., Choti, M.A., Hruban, R.H., Pawlik, T.M., and Wolfgang, C.L. (2014). 2564 resected periampullary adenocarcinomas at a single institution: trends over three decades. HPB *16*, 83–90.

42. Allen, P.J., Kuk, D., Castillo, C.F.D., Basturk, O., Wolfgang, C.L., Cameron, J.L., Lillemoe, K.D., Ferrone, C.R., Morales-Oyarvide, V., He, J., et al. (2017). Multi-institutional validation study of the American joint commission on cancer (8th edition) changes for T and N staging in patients with pancreatic adenocarcinoma. Ann. Surg. *265*, 185–191.

43. Hill, C.S., Rosati, L.M., Hu, C., Fu, W., Sehgal, S., Hacker-Prietz, A., Wolfgang, C.L., Weiss, M.J., Burkhart, R.A., Hruban, R.H., et al. (2022). Neoadjuvant stereotactic body radiotherapy after upfront chemotherapy improves pathologic outcomes compared with chemotherapy alone for patients with borderline resectable or locally advanced pancreatic adenocarcinoma without increasing perioperative toxicity. Ann. Surg Oncol. *29*, 2456–2468. https://doi.org/10.1245/s10434-021-11202-8.

44. Park, W., Chawla, A., and O'Reilly, E.M. (2021). Pancreatic cancer: a review. JAMA *326*, 851–862.

45. Neesse, A., Algül, H., Tuveson, D.A., and Gress, T.M. (2015). Stromal biology and therapy in pancreatic cancer: a changing paradigm. Gut *64*, 1476–1484.

46. Maloney, E., DuFort, C.C., Provenzano, P.P., Farr, N., Carlson, M.A., Vohra, R., Park, J., Hingorani, S.R., and Lee, D. (2019). Non-invasive monitoring of stromal biophysics with targeted depletion of hyaluronan in pancreatic ductal adenocarcinoma. Cancers *11*, 772.

47. Torphy, R.J., Fujiwara, Y., and Schulick, R.D. (2020). Pancreatic cancer treatment: better, but a long way to go. Surg. Today *50*, 1117–1125.

48. Noë, M., Rezaee, N., Asrani, K., Skaro, M., Groot, V.P., Wu, P.H., Olson, M.T., Hong, S.M., Kim, S.J., Weiss, M.J., et al. (2018). Immunolabeling of cleared human pancreata provides insights into three-dimensional pancreatic anatomy and pathology. Am. J. Pathol. *188*, 1530–1535.

49. Vieites-Prado, A., and Renier, N. (2021). Tissue clearing and 3D imaging in developmental biology. Development *148*, dev199369.

50. Richardson, D.S., Guan, W., Matsumoto, K., Pan, C., Chung, K., Ertürk, A., Ueda, H.R., and Lichtman, J.W. (2021). Tissue clearing. Nat. Rev. Methods Primers *1*, 84.

51. Hong, S.M., Jung, D., Kiemen, A., Gaida, M.M., Yoshizawa, T., Braxton, A.M., Noë, M., Lionheart, G., Oshima, K., Thompson, E.D., et al. (2020). Three-dimensional visualization of cleared human pancreas cancer reveals that sustained epithelial-to-mesenchymal transition is not required for venous invasion. Mod. Pathol. *33*, 639–647.

52. Kiemen, A.L., Braxton, A.M., Grahn, M.P., Han, K.S., Babu, J.M., Reichel, R., Jiang, A.C., Kim, B., Hsu, J., Amoa, F., et al. (2022). CODA: quantitative 3D reconstruction of large tissues at cellular resolution. Nat. Methods *19*, 1490–1499.

53. Schiffer, C., Spitzer, H., Kiwitz, K., Unger, N., Wagstyl, K., Evans, A.C., Harmeling, S., Amunts, K., and Dickscheid, T. (2021). Convolutional neural networks for cytoarchitectonic brain mapping at large scale. Neuroimage *240*, 118327.

54. Tward, D., Brown, T., Kageyama, Y., Patel, J., Hou, Z., Mori, S., Albert, M., Troncoso, J., and Miller, M. (2020). Diffeomorphic registration

with intensity transformation and missing data: application to 3D digital pathology of alzheimer's disease. Front. Neurosci. *14*, 52.

55. Kugler, M., Goto, Y., Tamura, Y., Kawamura, N., Kobayashi, H., Yokota, T., Iwamoto, C., Ohuchida, K., Hashizume, M., Shimizu, A., and Hontani, H. (2019). Robust 3D image reconstruction of pancreatic cancer tumors from histopathological images with different stains and its quantitative performance evaluation. Int. J. Comput. Assist. Radiol. Surg. *14*, 2047–2055.

56. Song, Y., Treanor, D., Bulpitt, A.J., and Magee, D.R. (2013). 3D reconstruction of multiple stained histology images. J. Pathol. Inform. *4*, S7.

57. Magee, D., Song, Y., Gilbert, S., Roberts, N., Wijayathunga, N., Wilcox, R., Bulpitt, A., and Treanor, D. (2015). Histopathology in 3D: from three-dimensional reconstruction to multi-stain and multi-modal analysis. J. Pathol. Inform. *6*, 6.

58. Alkemade, A., Bazin, P.L., Balesar, R., Pine, K., Kirilina, E., Möller, H.E., Trampel, R., Kros, J.M., Keuken, M.C., Bleys, R.L.A.W., et al. (2022). A unified 3D map of microscopic architecture and MRI of the human brain. Sci. Adv. *8*, eabj7892.

59. Zhao, S., Todorov, M.I., Cai, R., Maskari, R.A., Steinke, H., Kemter, E., Mai, H., Rong, Z., Warmer, M., Stanic, K., et al. (2020). Cellular and molecular probing of intact human organs. Cell *180*, 796–812.e19.

60. Pothula, S.P., Xu, Z., Goldstein, D., Pirola, R.C., Wilson, J.S., and Apte, M.V. (2016). Key role of pancreatic stellate cells in pancreatic cancer. Cancer Lett. *381*, 194–200.

61. Molbay, M., Kolabas, Z.I., Todorov, M.I., Ohn, T.L., and Ertürk, A. (2021). A guidebook for DISCO tissue clearing. Mol. Syst. Biol. *17*, e9807.

62. Hong, S.M., Noë, M., Hruban, C.A., Thompson, E.D., Wood, L.D., and Hruban, R.H. (2019). A "clearer" view of pancreatic pathology: a review of tissue clearing and advanced microscopy techniques. Adv. Anat. Pathol. *26*, 31–39.

63. Hahn, M., Nord, C., Eriksson, M., Morini, F., Alanentalo, T., Korsgren, O., and Ahlgren, U. (2021). 3D imaging of human organs with micrometer resolution - applied to the endocrine pancreas. Commun. Biol. *4*, 1063.

64. Jailkhani, N., Ingram, J.R., Rashidian, M., Rickelt, S., Tian, C., Mak, H., Jiang, Z., Ploegh, H.L., and Hynes, R.O. (2019). Noninvasive imaging of tumor progression, metastasis, and fibrosis using a nanobody targeting the extracellular matrix. Proc. Natl. Acad. Sci. USA *116*, 14181–14190.

65. Chames, P., and Rothbauer, U. (2020). Special issue: nanobody. Antibodies *9*, 6.

66. Ramos-Gomes, F., Bode, J., Sukhanova, A., Bozrova, S.V., Saccomano, M., Mitkovski, M., Krueger, J.E., Wege, A.K., Stuehmer, W., Samokhvalov, P.S., et al. (2018). Single- and two-photon imaging of human micrometastases and disseminated tumour cells with conjugates of nanobodies and quantum dots. Sci. Rep. *8*, 4595.

67. Rousserie, G., Grinevich, R., Brazhnik, K., Even-Desrumeaux, K., Reveil, B., Tabary, T., Chames, P., Baty, D., Cohen, J.H.M., Nabiev, I., and Sukhanova, A. (2015). Detection of carcinoembryonic antigen using single-domain or full-size antibodies stained with quantum dot conjugates. Anal. Biochem. *478*, 26–32.

68. Croce, A.C., and Bottiroli, G. (2014). Autofluorescence spectroscopy and imaging: a tool for biomedical research and diagnosis. Eur. J. Histochem. *58*, 2461.

69. Hahn, M., Nord, C., Franklin, O., Alanentalo, T., Mettävainio, M.I., Morini, F., Eriksson, M., Korsgren, O., Sund, M., and Ahlgren, U. (2020). Mesoscopic 3D imaging of pancreatic cancer and Langerhans islets based on tissue autofluorescence. Sci. Rep. *10*, 18246.

70. Ariel, P. (2017). A beginner's guide to tissue clearing. Int. J. Biochem. Cell Biol. *84*, 35–39.

71. Tian, T., Yang, Z., and Li, X. (2021). Tissue clearing technique: recent progress and biomedical applications. J. Anat. *238*, 489–507.

72. Richardson, D.S., and Lichtman, J.W. (2015). Clarifying tissue clearing. Cell *162*, 246–257.

73. Pan, C., Cai, R., Quacquarelli, F.P., Ghasemigharagoz, A., Lourbopoulos, A., Matryba, P., Plesnila, N., Dichgans, M., Hellal, F., and Ertürk, A. (2016). Shrinkage-mediated imaging of entire organs and organisms using uDISCO. Nat. Methods *13*, 859–867.

74. Messal, H.A., Almagro, J., Zaw Thin, M., Tedeschi, A., Ciccarelli, A., Blackie, L., Anderson, K.I., Miguel-Aliaga, I., van Rheenen, J., and Behrens, A. (2021). Antigen retrieval and clearing for whole-organ immunofluorescence by FLASH. Nat. Protoc. *16*, 239–262.

75. Power, R.M., and Huisken, J. (2017). A guide to light-sheet fluorescence microscopy for multiscale imaging. Nat. Methods *14*, 360–373.

76. Sharpe, J., Ahlgren, U., Perry, P., Hill, B., Ross, A., Hecksher-Sørensen, J., Baldock, R., and Davidson, D. (2002). Optical projection tomography as a tool for 3D microscopy and gene expression studies. Science *296*, 541–545.

77. Viens, P., Thyss, A., Garnier, G., and Ayela, P. (1988). Thrombocytopenia, the acquired immunodeficiency syndrome (AIDS), and zidovudine. Ann. Intern. Med. *109*, 681.

78. Bayguinov, P.O., Oakley, D.M., Shih, C.C., Geanon, D.J., Joens, M.S., and Fitzpatrick, J.A.J. (2018). Modern laser scanning confocal microscopy. Curr. Protoc. Cytom. *85*, e39.

79. Helmchen, F., and Denk, W. (2005). Deep tissue two-photon microscopy. Nat. Methods *2*, 932–940.

80. Pan, C., Schoppe, O., Parra-Damas, A., Cai, R., Todorov, M.I., Gondi, G., von Neubeck, B., Böğürcü-Seidel, N., Seidel, S., Sleiman, K., et al. (2019). Deep learning reveals cancer metastasis and therapeutic antibody targeting in the entire body. Cell *179*, 1661–1676.e19.

81. Nirschl, J.J., Janowczyk, A., Peyster, E.G., Frank, R., Margulies, K.B., Feldman, M.D., and Madabhushi, A. (2018). A deep-learning classifier identifies patients with clinical heart failure using whole-slide images of H&E tissue. PLoS One *13*, e0192726.

82. Giesen, C., Wang, H.A.O., Schapiro, D., Zivanovic, N., Jacobs, A., Hattendorf, B., Schüffler, P.J., Grolimund, D., Buhmann, J.M., Brandt, S., et al. (2014). Highly multiplexed imaging of tumor tissues with subcellular resolution by mass cytometry. Nat. Methods *11*, 417–422.

83. Ho, W.J., Yarchoan, M., Charmsaz, S., Munday, R.M., Danilova, L., Sztein, M.B., Fertig, E.J., and Jaffee, E.M. (2020). Multipanel mass cytometry reveals anti-PD-1 therapy-mediated B and T cell compartment remodeling in tumor-draining lymph nodes. JCI Insight *5*, e132286.

84. Liu, Y., Yang, M., Deng, Y., Su, G., Enninful, A., Guo, C.C., Tebaldi, T., Zhang, D., Kim, D., Bai, Z., et al. (2020). High-spatial-resolution multi-omics sequencing via deterministic barcoding in tissue. Cell *183*, 1665–1681.e18.

85. Rao, A., Barkley, D., França, G.S., and Yanai, I. (2021). Exploring tissue architecture using spatial transcriptomics. Nature *596*, 211–220.

86. Korehisa, S., Ikeda, T., Okano, S., Saeki, H., Oki, E., Oda, Y., Hashizume, M., and Maehara, Y. (2018). A novel histological examination with dynamic three-dimensional reconstruction from multiple immunohistochemically stained sections of a PD-L1-positive colon cancer. Histopathology *72*, 697–703.

87. Black, S., Phillips, D., Hickey, J.W., Kennedy-Darling, J., Venkataraaman, V.G., Samusik, N., Goltsev, Y., Schürch, C.M., and Nolan, G.P. (2021). CODEX multiplexed tissue imaging with DNA-conjugated antibodies. Nat. Protoc. *16*, 3802–3835.

88. Allam, M., Hu, T., Cai, S., Laxminarayanan, K., Hughley, R.B., and Coskun, A.F. (2021). Spatially visualized single-cell pathology of highly multiplexed protein profiles in health and disease. Commun. Biol. *4*, 632.

89. Sabdyusheva Litschauer, I., Becker, K., Saghafi, S., Ballke, S., Bollwein, C., Foroughipour, M., Gaugeler, J., Foroughipour, M., Schavelová, V., László, V., et al. (2020). 3D histopathology of human tumours by fast clearing and ultramicroscopy. Sci. Rep. *10*, 17619.

90. Mai, H., Rong, Z., Zhao, S., Cai, R., Steinke, H., Bechmann, I., and Ertürk, A. (2022). Scalable tissue labeling and clearing of intact human organs. Nat. Protoc. *17*, 2188–2215.

91. Okuda, R., Gjeta, B., Popovic, D., Maynard, A., Yu, Q., He, Z., Santel, M., Seimiya, M., Morinaga, S., Miyagi, Y., et al. (2022). Reconstructing cell interactions and state trajectories in pancreatic cancer stromal tumoroids. Preprint at bioRxiv. https://doi.org/10.1101/2022.02.14.480334.

92. Drifka, C.R., Tod, J., Loeffler, A.G., Liu, Y., Thomas, G.J., Eliceiri, K.W., and Kao, W.J. (2015). Periductal stromal collagen topology of pancreatic ductal adenocarcinoma differs

from that of normal and chronic pancreatitis. Mod. Pathol. *28*, 1470–1480.

93. Xu, S., Xu, H., Wang, W., Li, S., Li, H., Li, T., Zhang, W., Yu, X., and Liu, L. (2019). The role of collagen in cancer: from bench to bedside. J. Transl. Med. *17*, 309.

94. Puls, T.J., Tan, X., Whittington, C.F., and Voytik-Harbin, S.L. (2017). 3D collagen fibrillar microstructure guides pancreatic cancer cell phenotype and serves as a critical design parameter for phenotypic models of EMT. PLoS One *12*, e0188870.

95. Drifka, C.R., Loeffler, A.G., Mathewson, K., Keikhosravi, A., Eickhoff, J.C., Liu, Y., Weber, S.M., Kao, W.J., and Eliceiri, K.W. (2016). Highly aligned stromal collagen is a negative prognostic factor following pancreatic ductal adenocarcinoma resection. Oncotarget *7*, 76197–76213.

96. Fraley, S.I., Wu, P.H., He, L., Feng, Y., Krisnamurthy, R., Longmore, G.D., and Wirtz, D. (2015). Three-dimensional matrix fiber alignment modulates cell migration and MT1-MMP utility by spatially and temporally directing protrusions. Sci. Rep. *5*, 14580.

97. Benias, P.C., Wells, R.G., Sackey-Aboagye, B., Klavan, H., Reidy, J., Buonocore, D., Miranda, M., Kornacki, S., Wayne, M., Carr-Locke, D.L., and Theise, N.D. (2018). Structure and distribution of an unrecognized interstitium in human tissues. Sci. Rep. *8*, 7610.

98. Hruban, R.H., Gaida, M.M., Thompson, E., Hong, S.M., Noë, M., Brosens, L.A., Jongepier, M., Offerhaus, G.J.A., and Wood, L.D. (2019). Why is pancreatic cancer so deadly? The pathologist's view. J. Pathol. *248*, 131–141.

99. Kayahara, M., Nakagawara, H., Kitagawa, H., and Ohta, T. (2007). The nature of neural invasion by pancreatic cancer. Pancreas *35*, 218–223.

100. Hruban, R.H., Takaori, K., Klimstra, D.S., Adsay, N.V., Albores-Saavedra, J., Biankin, A.V., Biankin, S.A., Compton, C., Fukushima, N., Furukawa, T., et al. (2004). An illustrated consensus on the classification of pancreatic intraepithelial neoplasia and intraductal papillary mucinous neoplasms. Am. J. Surg. Pathol. *28*, 977–987.

101. Basturk, O., Hong, S.M., Wood, L.D., Adsay, N.V., Albores-Saavedra, J., Biankin, A.V., Brosens, L.A.A., Fukushima, N., Goggins, M., Hruban, R.H., et al. (2015). A revised classification system and recommendations from the Baltimore consensus meeting for neoplastic precursor lesions in the pancreas. Am. J. Surg. Pathol. *39*, 1730–1741.

102. HuBMAP Consortium (2019). The human body at cellular resolution: the NIH Human Biomolecular Atlas Program. Nature *574*, 187–192.

103. Ruiz Tejada Segura, M.L., Abou Moussa, E., Garabello, E., Nakahara, T.S., Makhlouf, M., Mathew, L.S., Wang, L., Valle, F., Huang, S.S.Y., Mainland, J.D., et al. (2022). A 3D transcriptomics atlas of the mouse nose sheds light on the anatomical logic of smell. Cell Rep. *38*, 110547.

104. Casamitjana, A., Lorenzi, M., Ferraris, S., Peter, L., Modat, M., Stevens, A., Fischl, B., Vercauteren, T., and Iglesias, J.E. (2022). Robust joint registration of multiple stains and MRI for multimodal 3D histology reconstruction: application to the Allen human brain atlas. Med. Image Anal. *75*, 102265.

105. Walsh, C.L., Tafforeau, P., Wagner, W.L., Jafree, D.J., Bellier, A., Werlein, C., Kühnel, M.P., Boller, E., Walker-Samuel, S., Robertus, J.L., et al. (2021). Imaging intact human organs with local resolution of cellular structures using hierarchical phase-contrast tomography. Nat. Methods *18*, 1532–1541.

106. Weisberg, E.M., Fishman, E.K., Chu, L.C., and Catmull, E. (2021). Man versus machine? Radiologists and artificial intelligence work better together. J. Am. Coll. Radiol. *18*, 887–889.